Designs and Implementation for an Advanced Automated Manual Transmission System of Hybrid Electric Vehicles

Shih-Hsiang Chien* Chin-Hone Lin Pao-Cheng Lin
Mechanical and System Research Lab.
Industrial Technology Research Institute
Bldg. 58, 195 Chung Hsing Rd., Section 4, Chutung, Hsinchu, Taiwan
*Email: chiensh@itri.org.tw**
Tel:+886-3-5915932 Fax: +886-5820453

Abstract

A new type Automated Manual Transmission (AMT) control system, designed by model-base MATLAB/Sumulink platform, is applied to Hybrid Electrical Vehicles (HEVs). The drive of the AMT actuator motor is Permanent Magnet Synchronous Motor (PMSM), which is utilized and implemented according to preliminary simulation of a closed-loop control system. Compared with the DC brush motor, the PMSM has advantages of high efficiency and maintenance free. After system designs, a platform consisting of the control unit and the AMT system is established. Vehicle test results show that the high quality gear shifting period to be less than regular time, 1.2-1.4 second, by the new PMSM drive system.

Keywords: Permanent Magnet Synchronous Motor, Transmission System, Hybrid Electric Vehicle.

1 Introduction

On the basis of the globally increasing interests in the environmental concerns such as air pollution, acid rain, green-house effect, HEVs have become popular during past years. Comparing to traditional Internal Combustion Engine (ICE) vehicles, HEVs are characterized by many advantages such as low emission, low fuel consuming and also better performance.

For transmission systems, the AMT system can not only operate as efficiently as the manual transmission does but also can shift gear automatically as the automatic transmission does. In addition, the cost is lower than that of the automatic transmission. The AMT system is powered by hydraulic or electromechanical devices to shift gear. Generally, the actuator of the electromechanical gear shifting device adopted by the current AMT is a DC brush motor. However, DC brush motor is with spike issue and low durability which results in high maintenance frequency[1][2]. To solve this problem, this paper proposes a new AMT system for HEV based upon permanent magnet synchronous motor. Controller designs and platform tests are also discussed.

2 The Mathematical Model of the PMSM

The voltage and the current of the PMSM are time-variant and nonlinear signals, the mathematical model is a complex problem. In order to analyze easily, we simplify the model and transformed the three-phase frame into two-axis frame. Suppose that the motor is three-phase, two poles, balanced windings, symmetrical airgap, the loss of the eddy current and hysteresis is omitted[3][4], which is shown in Fig. 1. In the meaning of the coordinate transformation, the a-b-c frame and the $\alpha - \beta$ frame represent the three-phase stationary frame and the two axes reference frame respectively. The d-q frame stands for synchronously rotating frame of the rotor.

The equivalent circuit of the PMSM is displayed in Fig. 2, where v_{as} , v_{bs} , v_{cs} and i_{as} , i_{bs} , i_{cs} indicate the phase voltage and the phase current of the stator windings. The notations R_s and

L_{ss} signifies the resistance and the inductance of the stator, the symbol λ of the equation (2.4) denotes the stator flux linkage.

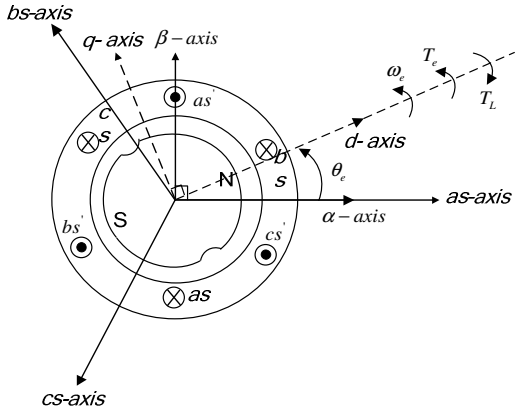

Fig. 1. Relationship between a-b-c and d-q

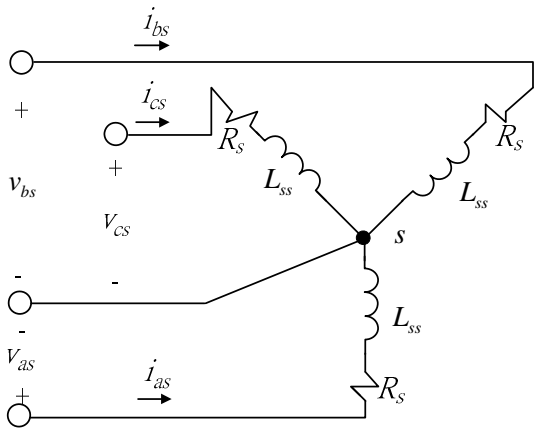

Fig. 2. The equipment circuit of the PMSM

Using the coupled circuit approach and motor notation, the voltage equations of the magnetically coupled stator circuits can be written as follows

$$v_{as} = R_s i_{as} + \frac{d}{dt}\lambda_{as} \tag{2.1}$$

$$v_{bs} = R_s i_{bs} + \frac{d}{dt}\lambda_{bs} \tag{2.2}$$

$$v_{cs} = R_s i_{cs} + \frac{d}{dt}\lambda_{cs} \tag{2.3}$$

The matrix form of the stator voltage equations are described as equation (2.4).

$$\begin{bmatrix} v_{as} \\ v_{bs} \\ v_{cs} \end{bmatrix} = \begin{bmatrix} R_s & 0 & 0 \\ 0 & R_s & 0 \\ 0 & 0 & R_s \end{bmatrix} \begin{bmatrix} i_{as} \\ i_{bs} \\ i_{cs} \end{bmatrix} + \begin{bmatrix} \frac{d}{dt}\lambda_{as} \\ \frac{d}{dt}\lambda_{bs} \\ \frac{d}{dt}\lambda_{cs} \end{bmatrix} \tag{2.4}$$

In the equation (2.4), the flux linkage equations are presented in the equation (2.5) to (2.7)

$$\lambda_{as} = L_{ss} i_{as} - \frac{1}{2} L_{ms} i_{bs} - \frac{1}{2} L_{ms} i_{cs} + \lambda_f \cos\theta_e \tag{2.5}$$

$$\lambda_{bs} = -\frac{1}{2} L_{ms} i_{as} + L_{ss} i_{bs} - \frac{1}{2} L_{ms} i_{cs} + \lambda_f \cos(\theta_e - \frac{2\pi}{3}) \tag{2.6}$$

$$\lambda_{cs} = -\frac{1}{2} L_{ms} i_{as} - \frac{1}{2} L_{ms} i_{bs} + L_{ss} i_{cs} + \lambda_f \cos(\theta_e + \frac{2\pi}{3}) \tag{2.7}$$

By utilizing the equation (2.1) to (2.7) and defining $p = \frac{d}{dt}$, $L_s = \frac{3}{2} L_{ms} + L_{ls}$, the voltage equations of the stator are exhibited,

$$\begin{bmatrix} v_{as} \\ v_{bs} \\ v_{cs} \end{bmatrix} = \begin{bmatrix} R_s + pL_s & 0 & 0 \\ 0 & R_s + pL_s & 0 \\ 0 & 0 & R_s + pL_s \end{bmatrix} \begin{bmatrix} i_{as} \\ i_{bs} \\ i_{cs} \end{bmatrix} + \begin{bmatrix} e_{as} \\ e_{bs} \\ e_{cs} \end{bmatrix} \tag{2.8}$$

where the notations e_{as} , e_{bs} , e_{cs} are induced voltage.

In order to analyze the coordinate transformation and discuss the motor mathematical model clearly, we firstly consider the relationship of the a-b-c frame and the $\alpha - \beta$ frame, which is illustrated with Fig. 3.

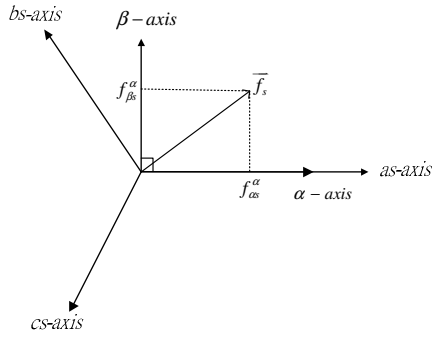

Fig. 3. Relationship between a-b-c and $\alpha - \beta$

Suppose that there is a vector $\vec{f}_s$ in the a-b-c frame. The vector may be voltage, current or flux linkage of the stator. It can be transformed into the $\alpha - \beta$ frame by equation (2.9), where c is a transformation constant.

$$\overline{f_s} = f_{\alpha s}^{\alpha} + j f_{\beta s}^{\alpha} = c\left(f_{as} + f_{bs} e^{j\frac{2}{3}\pi} + f_{cs} e^{-j\frac{2}{3}\pi} \right) \tag{2.9}$$

Hence, we choose the constant $c = \frac{2}{3}$ and substitute it into the above equation. The transformation

matrix with the a-b-c frame and the $\alpha-\beta$ frame can be obtained below.

$$\begin{bmatrix} f_{\alpha s}^{\alpha} \\ f_{\beta s}^{\alpha} \\ f_{0s}^{\alpha} \end{bmatrix} = \frac{2}{3}\begin{bmatrix} 1 & -\frac{1}{2} & -\frac{1}{2} \\ 0 & \frac{\sqrt{3}}{2} & -\frac{\sqrt{3}}{2} \\ \frac{1}{2} & \frac{1}{2} & \frac{1}{2} \end{bmatrix}\begin{bmatrix} f_{as} \\ f_{bs} \\ f_{cs} \end{bmatrix} \tag{2.10}$$

After analyzing the a-b-c frame and the $\alpha-\beta$ frame, the relationship between $\alpha-\beta$ axes and synchronously rotating frame is proposed in Fig. 4.

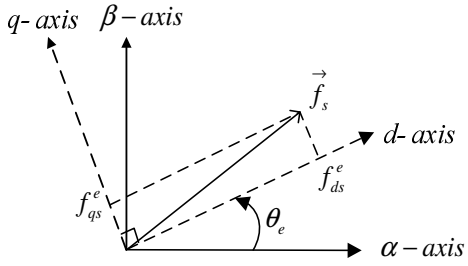

Fig. 4. Relationship between $\alpha-\beta$ and d-q

According to the Fig. 4, suppose that the vector $\vec{f}_s$ is defined as voltage, current or flux linkage. The relationship between d-q frame and $\alpha-\beta$ frame can be presented by equation (2.11), where θ_e is an electrical radian.

$$\begin{bmatrix} f_{ds}^e \\ f_{qs}^e \end{bmatrix} = \begin{bmatrix} \cos\theta_e & \sin\theta_e \\ -\sin\theta_e & \cos\theta_e \end{bmatrix}\begin{bmatrix} f_{\alpha s}^{\alpha} \\ f_{\beta s}^{\alpha} \end{bmatrix} \tag{2.11}$$

From the equation (2.9) to (2.11) and the above depictions, they can be easily transformed from three-phase stationary frame to synchronously rotating frame.

$$\begin{bmatrix} f_{ds}^e \\ f_{qs}^e \\ f_{0s}^e \end{bmatrix} = K_s \begin{bmatrix} f_{as} \\ f_{bs} \\ f_{cs} \end{bmatrix} \tag{2.12}$$

where

$$K_s = \frac{2}{3}\begin{bmatrix} \cos\theta_e & \cos(\frac{2}{3}\pi-\theta_e) & \cos(\frac{2}{3}\pi+\theta_e) \\ -\sin\theta_e & \sin(\frac{2}{3}\pi-\theta_e) & -\sin(\frac{2}{3}\pi+\theta_e) \\ \frac{1}{2} & \frac{1}{2} & \frac{1}{2} \end{bmatrix}$$

The expression for the electromagnetic torque developed by the machine can be obtained from the component of the input power that is transferred across the airgap. The total input power transferred into the machine is given by

$$P_{abc} = v_{as}i_{as} + v_{bs}i_{bs} + v_{cs}i_{cs} \tag{2.13}$$

When the stator phase quantities are transformed to the rotor d-q reference frame and considering the zero-sequence current is zero, the electromechanical power becomes

$$P_m = \frac{3}{2}\omega_m(\lambda_{ds}^e i_{qs}^e - \lambda_{qs}^e i_{ds}^e + \lambda_f^e i_{qs}^e) \tag{2.14}$$

For a P-pole machine, $\varpi_m = \frac{P}{2}\varpi_e$, with ϖ_e being the rotor speed in mechanical radian. Thus, equation (2.14) for a P-pole machine can also be written as

$$P_e = \frac{3}{2}\frac{P}{2}\omega_e(\lambda_{ds}^e i_{qs}^e - \lambda_{qs}^e i_{ds}^e + \lambda_f^e i_{qs}^e) \tag{2.15}$$

Dividing the electromechanical power by the mechanical speed of the rotor, the electromechanical torque developed by a P-pole machine can be expressed as the following equation.

$$T_e = \frac{P_e}{\omega_e}$$

$$= \frac{3}{4}P(\lambda_{ds}^e i_{qs}^e - \lambda_{qs}^e i_{ds}^e + \lambda_f^e i_{qs}^e) \tag{2.16}$$

By using the equation $\lambda = Li$ and suppose that $L_d = L_q$, the equation (2.16) can be simplified.

$$T_e = \frac{3}{4}P\lambda_f^e i_{qs}^e \tag{2.17}$$

The above equations are described as the motor electrical parameters. Besides, the mechanical characteristic equation of the motor is shown below.

$$T_e = T_L + J_m\frac{d\omega_m}{dt} + B_m\omega_m$$

$$= T_L + \frac{2}{P}\left(J_m\frac{d\omega_e}{dt} + B_m\omega_e\right) \tag{2.18}$$

Therefore, by employing (2.8), (2.17), (2.18) and coordinate transformation, the block diagram of the PMSM in the synchronously rotating frame is plotted in Fig. 5.

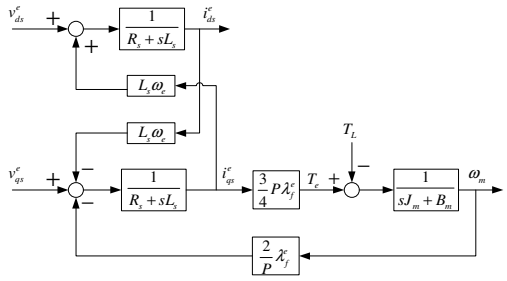

Fig. 5. The block diagram of the PMSM in the synchronously rotating frame

3 Design of the PMSM Controller

The control loops of the PMSM are composed of three close-loop systems, which are shown in Fig. 6. From the inner to the outer loops, there is q-axis stator current control, speed control and position control loops respectively. If the bandwidth of the inner loop is greater ten times than the outer loop, it can be separated into three independent loops. The block diagrams of the control scheme are displayed in Fig. 7~Fig. 9[6].

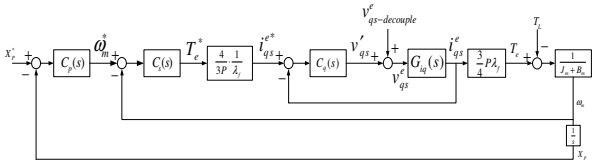

Fig. 6. The control loops of the PMSM

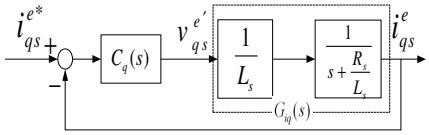

Fig. 7. The q-axis stator current control loop

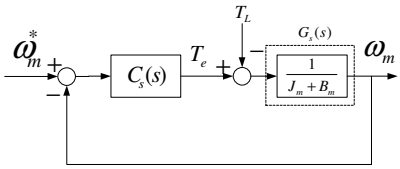

Fig. 8. The speed control loop

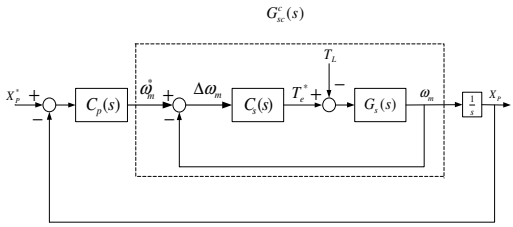

Fig. 9. The position control loop

From Fig. 7 to Fig. 9, transfer functions of the q-axis stator current control and speed control loop can be computed as

$$G_{iq}(s)=\frac{i_{qs}^{e}}{v_{qs}^{e'}}=\frac{1}{sL_s+R_s}=\frac{\frac{1}{L_s}}{s+\frac{R_s}{L_s}} \qquad (3.1)$$

$$G_s(s)=\frac{\varpi_m}{T_e-T_L}=\frac{1}{sJ_m+B_m}=\frac{\frac{1}{J_m}}{s+\frac{B_m}{J_m}} \qquad (3.2)$$

The (3.1) and (3.2) indicate that the differential equations of the mathematical model of control systems are all first order. In general, the Proportion- Integral (PI) controller can be designed to achieve the object of the motor control.

4 System Descriptions

The control block of an AMT system in HEVs are shown in Fig. 10, there are calibration tool, programming cable, CPU, power unit, power supply and motor. In this paper, the controlled system is designed by two parts. One is hardware including the key-on detection control circuit and the motor driving circuit of power unit; the other is operation system of software programs which were burned into CPU to operate the motor via calibration tool and programming cable. We proposed six transistors in the motor driving circuits and the control kernel of software, a dsPIC30F3010 Digital Signal Processor (DSP) of Microchip Company, through generating PWM control signals for the motor drives. The whole transmission systems can be fulfilled the purpose by driving circuits, programs, and other peripheral apparatus.

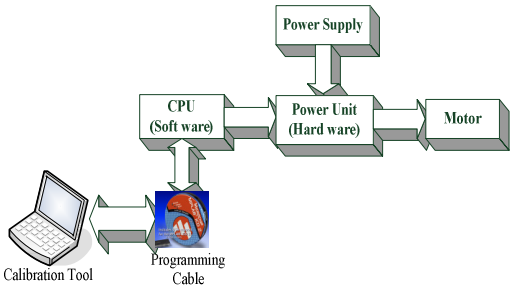

Fig. 10. The control block of an AMT system

The key-on detection control circuit in power unit supplies stable voltage to internal digital circuit of a controller U1 and external analog circuit of a sensor U2 which are designed as Fig. 11. U1 and U2 are low-drift linear voltage regulators. In order to prevent voltage drift, the output voltage of a regulator U2 must follows the output voltage of a regulator U1. If the transmission system switches to “key-on”, the transistor Q2 is connected, and then Q1 is also connected; therefore; the output voltage of battery can send to regulators U1 and U2 via Q1. The system is normally working. On the other

hand, the transistor Q2 will disconnect if the transmission system switches to “key-off”. In this case, the transistor Q3 will be connected to hold on power and keep Q1 connecting until important data are saved. After saving data, the controller disconnects the transistor Q3, and then Q1 turns to cut-off; as a result; the controller stops working.

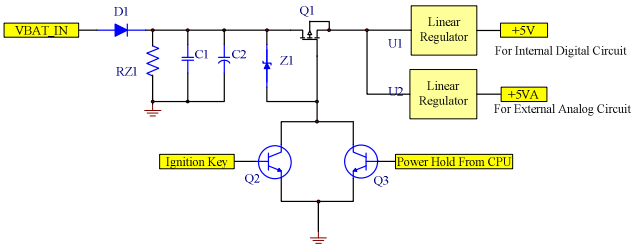

Fig. 11. The key-on detection control circuit

In this paper, two major tasks (5000Hz and 100Hz) are addressed to software operation system. The tasks can be called the Time-Base Tasks or Time-Triggered Tasks. In order to make use of CPU resources more efficiently, the decentralized concepts are presented. On the basis of 100Hz, there are three Sub-Rate Tasks utilized: 50Hz Task, 25Hz Task and 12.5Hz Task. Different Tasks have different purposes. The 500Hz Task is used to PMSM control programs. The 100Hz Task is for transmission system control strategy, motor speed calculation, communication and firmware calibration. Finally, the 50Hz Task, 25Hz Task and 12.5Hz Task are all applied to the diagnostics and protection firmware.

The following introduction will present operation system program of software and the control strategy for motor drives shown in Fig. 12. The purpose of designed software interruption is to trigger 5000Hz Task per 200 μs . Every 10ms will trigger one times in Background Tasks. The running time of 5000 Hz Task, no more than 200 μs , runs all Tasks no more than 10ms. We divide the Background Tasks into four parallel states: 100Hz Task, 50Hz Task, 25Hz Task and 12.5Hz Task. The running program is from high Task to low Task in sequence and only one Task can be run for every 10ms trigger in Background Tasks.

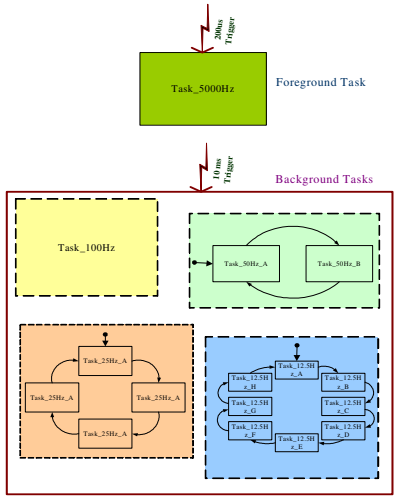

Fig. 12. The control strategy for motor driving

5 Experiment Results

The Automated clutch Manual Transmission (AcMT) system is defined as the AMT system with an actuator, the electric-clutch, in HEVs. It is developed by the Mechanical and System Research Lab of the ITRI as displayed in Fig. 13 and Fig. 14. For the application of HEVs, a practical motor driving circuit is shown in Fig. 15, and circuit components are designed as R1=10kΩ and R2=1kΩ.

Fig. 13. The Automated clutch Manual Transmission

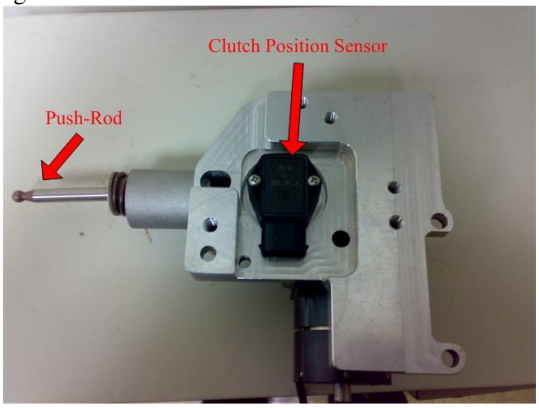

Fig. 14. The clutch actuator

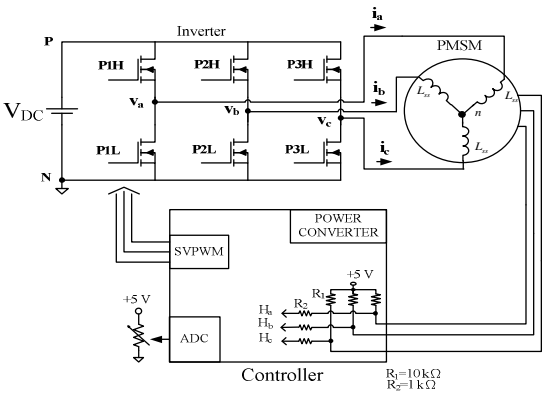

Fig. 15. The motor driving circuit

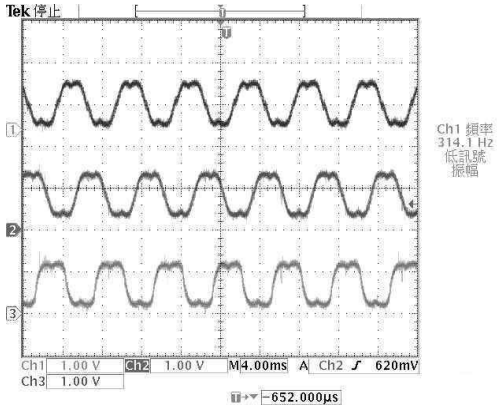

Fig. 16. The back-electromotive force of the PMSM

In order to check the waveform of vector control, we adjust PMSM speed to 2500rpm and observe its back-electromotive force. Hence, the phase voltages V_a, V_b, and V_c pass through low pass filter and the cut off frequency is 1KHz, the waveforms are shown in Fig. 16. While the motor speed is 800rpm through the line voltage V_{ab} of the closed-loop speed control, currents i_a and i_b are displayed in Fig. 17, and the phase current magnitude is 20A per unit. Fig. 18 illustrates that the hall sensor signal and three phase back-electromotive force. The channel 1 is the hall sensor signal of a-phase H_a, and the channel 2 to the channel 4 is the phase voltage V_{an}, V_{bn}, V_{cn}. The waveform of three phase hall sensor signals are also exhibited in Fig. 19, where the channel 1 to the channel 3 is the a-phase, b-phase and c-phase hall sensor signal respectively.

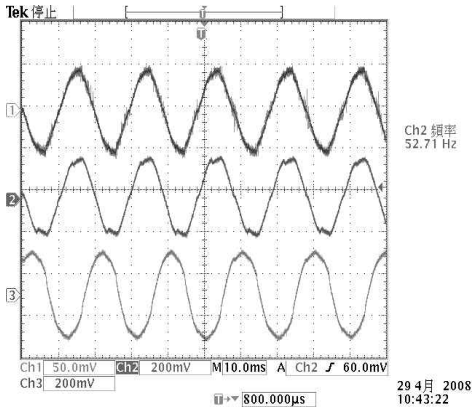

Fig. 17. V_{ab}, i_a and i_b of the PMSM

According to the design procedure, Fig. 20 to Fig. 22 displays three conditions: the position of push-rod from 30 to 180, from 30 to 230 and from 230 to 30; and the time periods are 0.322sec., 0.426sec. and 0.428sec. On the other hand, the time of clutch from release state to engage state is 0.426sec and reversely 0.428sec in opposite way. In general, the regulation of gear shifting period of an AMT vehicle is 1.2 sec. to 1.4sec. Therefore, the room for shifting time is equal to the summation of clutch engage/release times subtracted from gear shifting period. It will be 0.346 sec. to 0.546 sec. which is easy to be achieved.

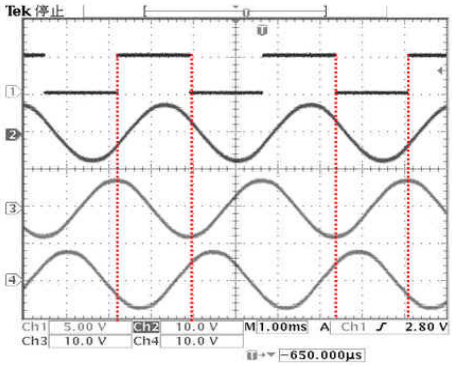

Fig. 18. The hall sensor signal and three phase back-electromotive force

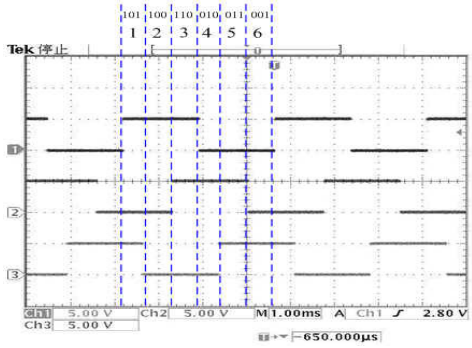

Fig. 19. The waveform of three phase hall sensor signals

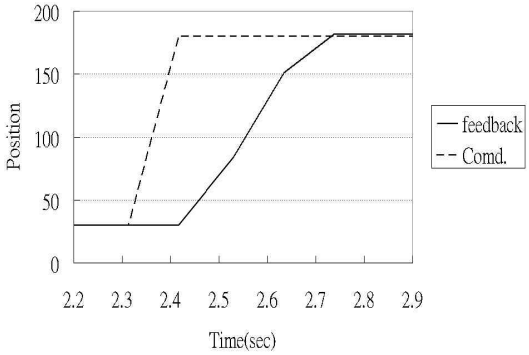

Fig. 20. The position of push-rod from 30 to 180

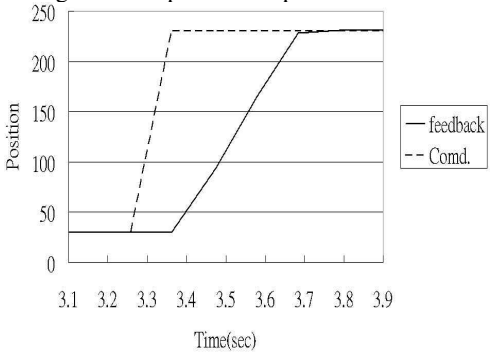

Fig. 21. The position of push-rod from 30 to 230

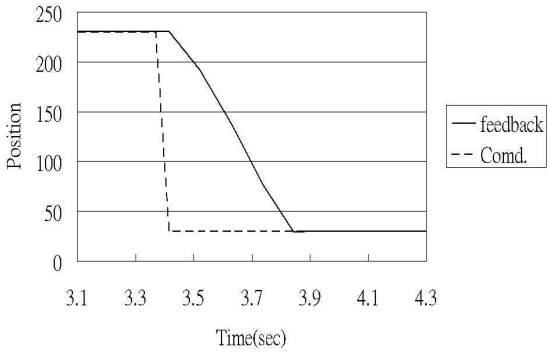

Fig. 22. The position of push-rod from 230 to 30

6 Conclusions

The paper aims to develop a driving circuits and software for PMSM based on dsPIC30F3010 Digital Signal Processor (DSP) by Microchip Company to implement the position control of e-clutch in the transmission system through PWM functionality. The design of the Proportion-Integral controller is successfully proposed to the motor control of the clutch. The PMSM controlled system utilizes the position and speed feedback mechanisms. Since there is no current feedback scheme, the hardware size and the cost can be reduced greatly.

The experiment results clearly show that not only an advanced AMT system of HEV can be implemented, but also the gear shifting period is less than 1.2 sec.

References

[1] Y. J. Chen, "The development of the AcMT technology," *The Journal of the mechanical industry, No. 260, 238~247*, Nov, 2004.

[2] Y. J. Chen, "The developing trend of the AMT," *The Journal of the mechanical industry, No. 248, 111~121,* Nov, 2003.

[3] B. K. Bose, "Modern power electronics and ac drives," Prentice Hall, N.J., 2001.

[4] C. M. Ong, "Dynamic simulation of electric machinery: using MATLAB/SIMULINK," N.J. :Prentice Hall PTR, 1998.

[5] C. M. Ong, "Dynamic simulation of electric machinery," Pearson Education Taiwan Ltd., Taiwan, 2003.

[6] C. H. Liu, "The alternating current machine control: The vector control and the direct torque control principle," 4th edition, Tung Hua Ltd., Taiwan, 2008.

Authors

Shih-Hsiang Chien, His research interests are in the area of variable structure systems, nonlinear control, adaptive control and fuzzy control theory. Currently, he is a researcher at Intelligent Mobility Tech. Division, ITRI, Taiwan.

Chin-Hone Lin, His main research interests are in the transmission system of the mobile and the hub motor control. Currently, he is a associate researcher at Intelligent Mobility Tech. Division, ITRI, Taiwan.

Pao-Cheng Lin, His area of interest includes power electronics and drives, the control of the power machines. Currently, he is a associate researcher at Intelligent Mobility Tech. Division, ITRI, Taiwan.